Dual Wavelength Electroluminescence from CdSe/CdS Tetrapods

ARTICLE *in* ACS NANO · FEBRUARY 2014

Impact Factor: 12.88 · DOI: 10.1021/nn500030t · Source: PubMed

Dual Wavelength Electroluminescence from CdSe/CdS Tetrapods

Jen It Wong,[†,#] Nimai Mishra,[‡,#] Guichuan Xing,[§,⊥] Mingjie Li,[‡] Sabyasachi Chakrabortty,[‡] Tze Chien Sum,[§,⊥] Yumeng Shi,[†] Yinthai Chan,[‡,∥,*] and Hui Ying Yang[†,*]

[†]Pillar of Engineering Product Development, Singapore University of Technology and Design, 20 Dover Drive, Singapore 138682, [‡]Department of Chemistry, National University of Singapore, 3 Science Drive 3, Singapore 117543, [§]School of Physical & Mathematical Sciences, Nanyang Technological University, 21 Nanyang Link, Singapore 637371, [⊥]Singapore—Berkeley Research Initiative for Sustainable Energy, 1 Create Way, Singapore 138602, and [∥]Institute for Materials Research & Engineering, A*STAR, 3 Research Link, Singapore 117602. [#]J.I.W. and N.M. contributed equally.

ABSTRACT We fabricated a single active layer quantum dot light-emitting diode device based on colloidal CdSe (core)/CdS (arm) tetrapod nanostructures capable of simultaneously producing room temperature electroluminesence (EL) peaks at two spectrally distinct wavelengths, namely, at ~500 and ~660 nm. This remarkable dual EL was found to originate from the CdS arms and CdSe core of the tetrapod architecture, which implies that the radiative recombination of injected charge carriers can independently take place at spatially distinct regions of the tetrapod. In contrast, control experiments employing CdSe-core-seeded CdS nanorods showed near-exclusive EL from the CdSe core. Time-resolved spectroscopy measurements on tetrapods revealed the presence of hole traps, which facilitated the localization and subsequent radiative recombination of excitons in the CdS arm regions, whereas excitonic recombination in nanorods took place predominantly within the vicinity of the CdSe core. These observations collectively highlight the role of morphology in the achievement of light emission from the different material components in heterostructured semiconductor nanoparticles, thus showing a way in developing a class of materials which are capable of exhibiting multiwavelength electroluminescence.

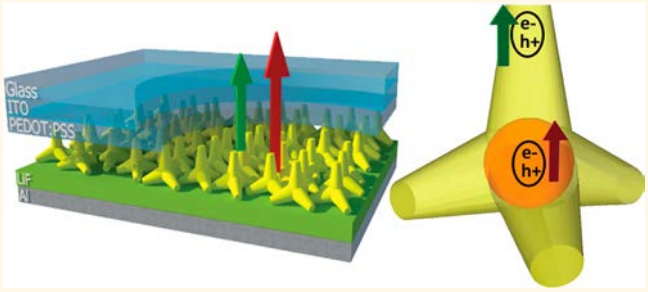

KEYWORDS: electroluminescence · light-emitting devices · CdSe · CdS · tetrapod nanocrystals · dual emission · colloidal nanocrystals

Recently, a large amount of attention has been given to the development of efficient semiconductor-based light sources as alternative lighting devices to lower energy consumption and reduce the carbon footprint. Among the many sources of lighting, light-emitting diodes (LEDs) are perhaps one of the most promising given that they offer excellent brightness, long operational lifetimes, low power consumption, and minimal maintenance.[1,2] The introduction of LEDs based on colloidal quantum dots (QDs) has promised not only a wide range of emission wavelengths with superior color saturation for ultrathin displays but also solution processability, which has since stimulated intensive experimental and theoretical investigation.[3−8] Following its inception in 1994,[9] quantum dot light-emitting diodes (QD-LEDs) have progressed from the use of CdSe cores embedded in a polymer blend sandwiched between two electrodes[10] to a monolayer of core-alloyed shell CdSe/CdZnS QDs within an OLED architecture.[11] The parameters which govern the performance of QD-LED devices using organic thin films as charge transport layers have also been investigated in detail, such as fluorescent resonance energy transfer (FRET)-dominated QD excitation,[12−14] nonradiative Auger recombination in charged QDs,[12] and efficiency roll-off *via* electric field-induced photoluminescence (PL) quenching.[15] The introduction of QDs with novel composition and dimensionality has also augmented the performance of QD-LEDs. For instance, thick-shell CdSe/CdS nanocrystals (≥13 CdS monolayers) have been chemically synthesized and employed as a high-performance active layer,[4] while highly ordered arrays of CdSe-seeded CdS nanorods have been utilized as polarized LED sources that cannot be readily achieved *via* the use of spherical QDs.[16,17]

Heterostructured semiconductor nanoparticles with distinct regions of different

* Address correspondence to chmchany@nus.edu.sg, yanghuiying@sutd.edu.sg.

Received for review January 3, 2014 and accepted February 23, 2014.

Published online February 23, 2014
10.1021/nn500030t

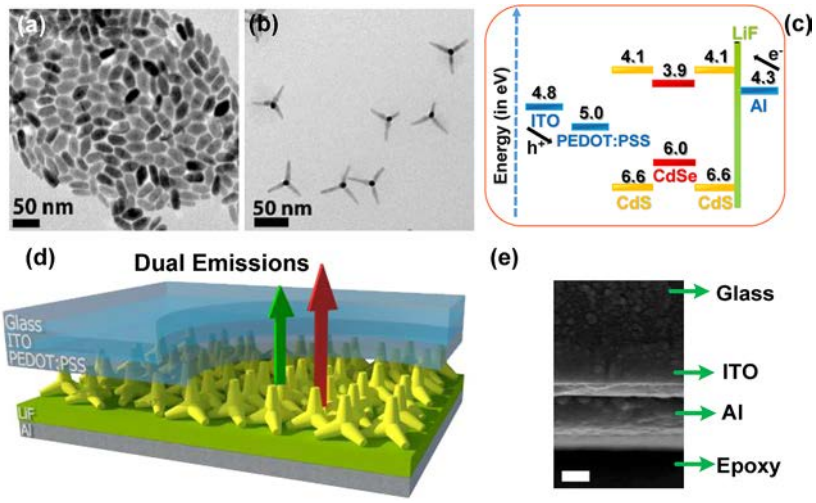

Figure 1. Low-resolution TEM images of CdSe-seeded CdS nanoheterostructures: (a) nanorods ~39 nm in length with ~15 nm diameter; (b) tetrapods ~27 nm in each arm length. (c) Corresponding band diagram of the active materials (CdSe-seeded CdS nanostructures) with respect to the electrode configuration. (d) Three-dimensional schematic view of the light-emitting device configuration where the active semiconductor nanoparticle layer (in this case, we have used tetrapods as an example) relative to the substrate, electron/hole injecting contacts, and charge transport layers are shown. (e) Cross-sectional SEM image of the device, where the substrate and electrode layers are evident. The scale bar is 100 nm.

material composition are interesting because they potentially allow for multiple wavelengths of emission due to radiative excitonic recombination in the different material regions.[18,19] With respect to nanoparticle-based LEDs, such multiple wavelength-emitting nanoparticles can increase the color range afforded by a subpixel (which typically comprises blue-, green-, or red-emitting QDs) or minimize the distance between different color-emitting subpixels. While extensive research has been carried out on the synthesis and physical characterization of CdSe/CdS tetrapod structures,[18,20−22] studies on their electroluminescence properties have been rare, if any. In this work, we develop a novel QD-LED which employs CdSe-seeded CdS tetrapods as the active material. We demonstrate that these tetrapod-based LEDs can simultaneously display electroluminescence (EL) at spectrally distinct wavelengths of ~660 and ~500 nm, which is attributed to radiative recombination in the CdSe core and CdS arms, respectively. Given the type I band alignment between the large CdSe core and CdS arms, an extremely fast localization of excitons from CdS to CdSe is expected, with subsequent radiative recombination taking place primarily within the CdSe core.[21] The occurrence of strong dual wavelength EL is therefore highly intriguing and is rationalized *via* an efficient hole trapping mechanism[23] in which excitons generated sufficiently far from the CdSe core remain localized in the CdS arm region long enough to undergo radiative recombination.

In order to investigate the potential of semiconductor nanoheterostructures as multiwavelength emitters within an LED device, rod-like and tetrapod-like CdSe-seeded CdS nanoparticles were synthesized *via* the seeded growth approach in which wurtzite and zinc blende CdSe (w- and zb-CdSe) cores were used as seeds, respectively.[21,24,25] This resulted in relatively monodisperse ~15 nm diameter nanorods about ~39 nm in length and tetrapods with an average arm length of ~27 nm, as illustrated in Figure 1a,b, respectively. Characterization of their emission profiles *via* a spectrofluorometer showed single peak PL centered at ~653 nm for nanorods and ~646 nm in the case of tetrapods. From UV−vis absorption spectra, the band gap energies of the CdSe core and CdS shell were determined, and a coarse alignment of the band gap with respect to the vacuum level was carried out by using previously established energy values of the valence band edge states of these nanoparticles.[26] These determined values served as motivation for the use of Al/LiF as the electron injecting contacts, while ITO/PEDOT:PSS was used as the hole injecting source. Figure 1c depicts the energy offsets of the components within the QD-LED device used for this study and provides a rationale for our adopted architecture. Figure 1d is a cartoon schematic describing the active semiconductor nanoparticle layer (in this case, we have used tetrapods as an example) relative to the substrate, electron/hole injecting contacts, and charge transport layers. Cross-sectional field emission scanning electron microscopy (FESEM) was used to determine the approximate thicknesses of the electrode and active layers in the actual device, as illustrated in Figure 1e. It should be noted that the thickness of the active layer was typically in the range of ~60 to ~100 nm, which may be considered as multiple monolayers of shape anisotropic semiconductor nanoparticles randomly close-packed into a film.

Electroluminescence was observed at an applied forward bias between 3.5 and 4.5 V in the case of the

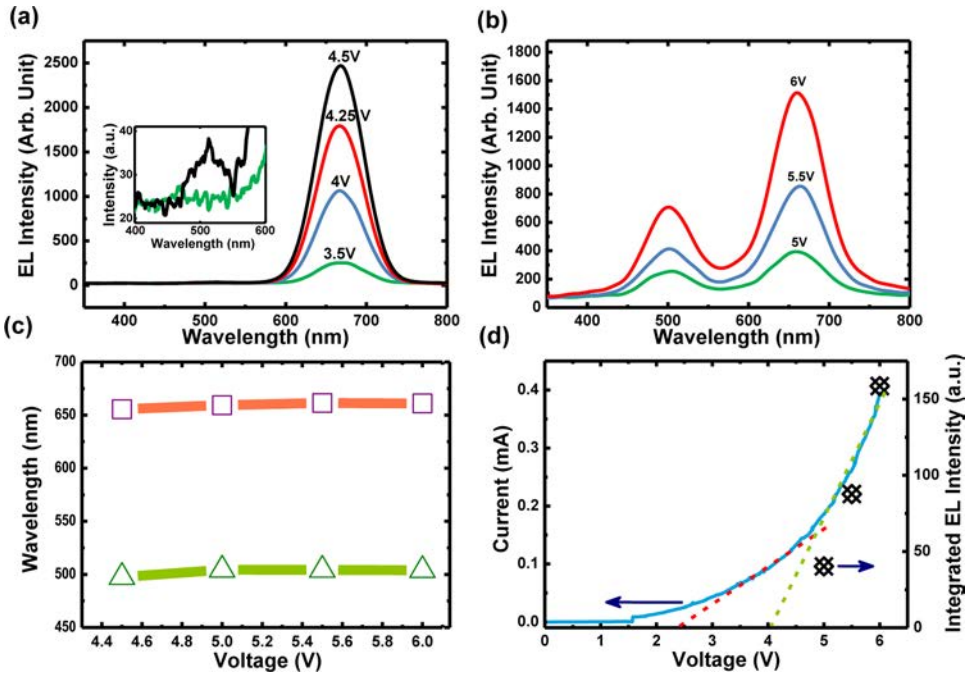

Figure 2. Electroluminescence spectra under different applied bias for CdSe-seeded CdS (a) nanorods and (b) tetrapods. (c) Fitted peaks from the EL spectrum of tetrapods at different voltages. (d) Current–voltage characteristic of the LED where tetrapods is the active layer. The scattered points show the integrated EL intensity.

CdSe-seeded CdS nanorod-based LEDs, as illustrated in Figure 2a, where a single emission peak centered at ~668 nm is prominently featured. This EL is attributed to radiative excitonic recombination in the CdSe core, which is consistent with PL derived from optical excitation under low pump fluence.[21] Closer inspection of the EL spectrum of nanorod-based LEDs revealed a barely perceptible peak at ~500 nm at an applied bias of 4.5 V and higher, which suggests that a very small fraction of the excitons injected recombine radiatively in the CdS shell. Surprisingly, EL peaks of comparable intensity centered at ~504 and ~661 nm were observed at similar applied bias in the case of the tetrapod-based LEDs, as depicted in Figure 2b. The fitted peak positions of the two emission wavelengths as a function of applied voltage are given in Figure 2c, where it is seen that there is essentially no red shift in the emission as the bias is increased. Within the range of bias applied, the presence of the quantum-confined Stark effect (QCSE), which has previously been shown to cause field-dependent spectral shifts in QDs,[27] may thus be ruled out. A current *versus* voltage (*I*–*V*) analysis of the tetrapod LED device was carried out, and the onset voltage of the blue and red emission wavelengths was determined by extrapolating the curvature along the measured *I*–*V* curve. The combined integrated EL intensity of both wavelengths between 5.0 and 6.0 V is also plotted on the same graph, where a relatively good correlation between increased current and increased EL intensity is observed. This implies that the emission obtained indeed derives from excitons formed *via* electron/hole injection from the electrodes.

RESULTS AND DISCUSSION

The appearance of two spectrally distinct wavelengths from CdSe-seeded CdS tetrapods under electrical excitation conditions is highly intriguing and warrants further investigation. As a precautionary measure, control experiments were performed to rule out the possibility that the CdS arms had detached from the tetrapod during the fabrication of the LED device. The w-CdSe and zb-CdSe cores used are about ~5.5 and ~5.4 nm in diameter, respectively, which should have a type I band alignment with the CdS shell.[28] Given the large size of the CdS shell, the absorption cross section at excitation energies larger than the CdS band gap is dominated by the shell. Due to the type I core–shell configuration, excitons generated in CdS are rapidly localized in the CdSe core, whereupon radiative recombination takes place. Prior work by Lutich *et al.* showed that the optical excitation of type I CdSe-seeded CdS tetrapods using 150 fs pulses at pump fluences on the order of 100 μJ cm^{-2} produced significant dual emission from both the CdSe core and CdS arms. It was argued that strong emission from the CdS arm was due to the CdSe core being saturated with a high density of excitons such that the driving force for excitons generated in CdS to relax into the CdSe core was removed, thus allowing radiative recombination to take place in CdS.[18] Figure 3a,b shows the respective PL spectra of the nanorods and tetrapods synthesized in this work under different pump intensities using 400 nm excitation pulses at a 1 kHz repetition rate and ~150 fs pulse duration from a frequency-doubled Ti:sapphire laser. It is readily seen

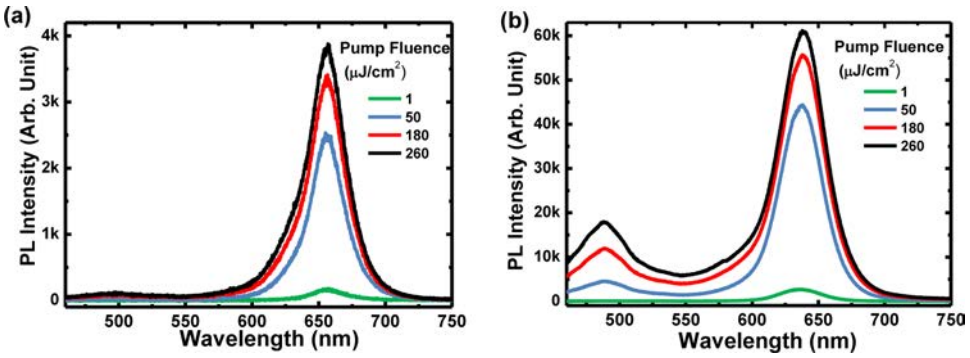

Figure 3. Photoluminescence spectra of CdSe-seeded CdS (a) nanorods and (b) tetrapods using 400 nm excitation pulses under different pump fluences.

that, at high pump intensities, significant dual wavelength PL may be seen in CdSe-seeded CdS tetrapods. On the other hand, CdSe-seeded CdS nanorods did not yield any appreciable dual wavelength emission even at large pump intensities, which may be attributed to their comparatively higher Auger recombination rate and lower absorption cross section at the pump wavelength.[18]

Under the relatively low optical pump intensities akin to the typical rates of electron/hole injection in an LED device, a relatively weak CdS PL was observed in the case of CdSe-seeded CdS tetrapods (see Supporting Information). This is in agreement with the findings of Lutich *et al.*, where weak emission from CdS which increased linearly with pump fluence was also observed at low excitation intensities.[18] However, given that the CdSe core hole states are not saturated at such low pump fluence, the appearance of the weak CdS emission peak in the type I tetrapod sample cannot be explicated by the exciton blocking effect as described above. Accordingly, such an explanation cannot be used to rationalize how the EL spectrum of tetrapods shows CdS arm emission nearly equivalent to that of the CdSe core in terms of intensity.

To resolve this conundrum on the observation of EL and PL from CdS in tetrapods at low pump intensity (*i.e.*, before core states are filled), we considered a recent observation by Wu *et al.* in which quasi-type II bulged CdSe-seeded CdS nanorods were found to possess three spatially separated long-lived exciton states.[29] It was proposed that these excitonic states were localized in and near the CdSe core, as well as near the surface of the CdS rod-like shell. The average probability for the formation of each of these exciton states is governed by a competition between the band offset driven hole localization to the CdSe seed and hole trapping at the CdS surface.[29,30] Our earlier findings of a fast hole trapping process to the CdS nanorod surface states in seeded quasi-type II CdSe/CdS nanodot/nanorod heterostructures were also consistent with these results by Wu *et al.* The decay lifetimes of these surface hole trap states also increase with increasing rod length or nanorod surface area.[23] Hence, we surmised that in the case of the type I tetrapods used in this work, the photogenerated holes in the CdS arm have a certain probability of being localized in surface trap states before reaching the CdSe core. There should therefore be at least two distinct long-lived excitons that can be formed upon optical excitation that is attributed to excitons in the CdSe core and CdS surface. In the case of type I CdSe/CdS nanorods, exciton localization to the CdSe core is expected to be the dominant process upon photogeneration of excitons in the CdS rod due to its smaller surface area.

Transient absorption (TA) measurements were carried out to validate the hypotheses stated above. Figure 4a,b shows the differential transmission ($\Delta T/T$) spectra of CdSe/CdS nanorods and tetrapods at a probe delay of 5 ps following a 400 nm pulse excitation. The two photobleaching (PB) bands (*i.e.*, $\Delta T/T > 0$) denoted as Y_O and X_O observed in the two arise from the state-filling of the photogenerated carriers in the CdS rod-like shell/arms and the carrier localization to the CdSe core, respectively. The larger amplitude ratio of Y_O to X_O in the tetrapods is due to the increased collective absorption from the CdS arms. The cartoon insets illustrate the different excitons formed in each nanoheterostructure upon photoexcitation. Figure 4c, d depicts the normalized bleach decay and formation kinetics monitored at the peaks of the Y_O and X_O PB bands in the nanorod and tetrapod samples, respectively. For the tetrapod sample, the buildup of the bleach transient of X_O is simultaneously matched with a fast decay of the Y_O bleach. These processes occur within ~1.5 ps, which reflects the carrier localization time from the CdS arm to the CdSe core. From the amplitude of the fast decay component of Y_O bleach, it may be estimated that about half the number of initially generated holes in CdS localize in the CdSe core while the remainder are trapped in surface states which accounts for the slow component of the Y_O bleach decay (~13 ns) as shown in Figure 4e.[23] This fitted decay time is consistent with the measured PL lifetime of ~10.5 ns for CdS emission as exemplified in Figure 4f, which is in the range of the reported emission

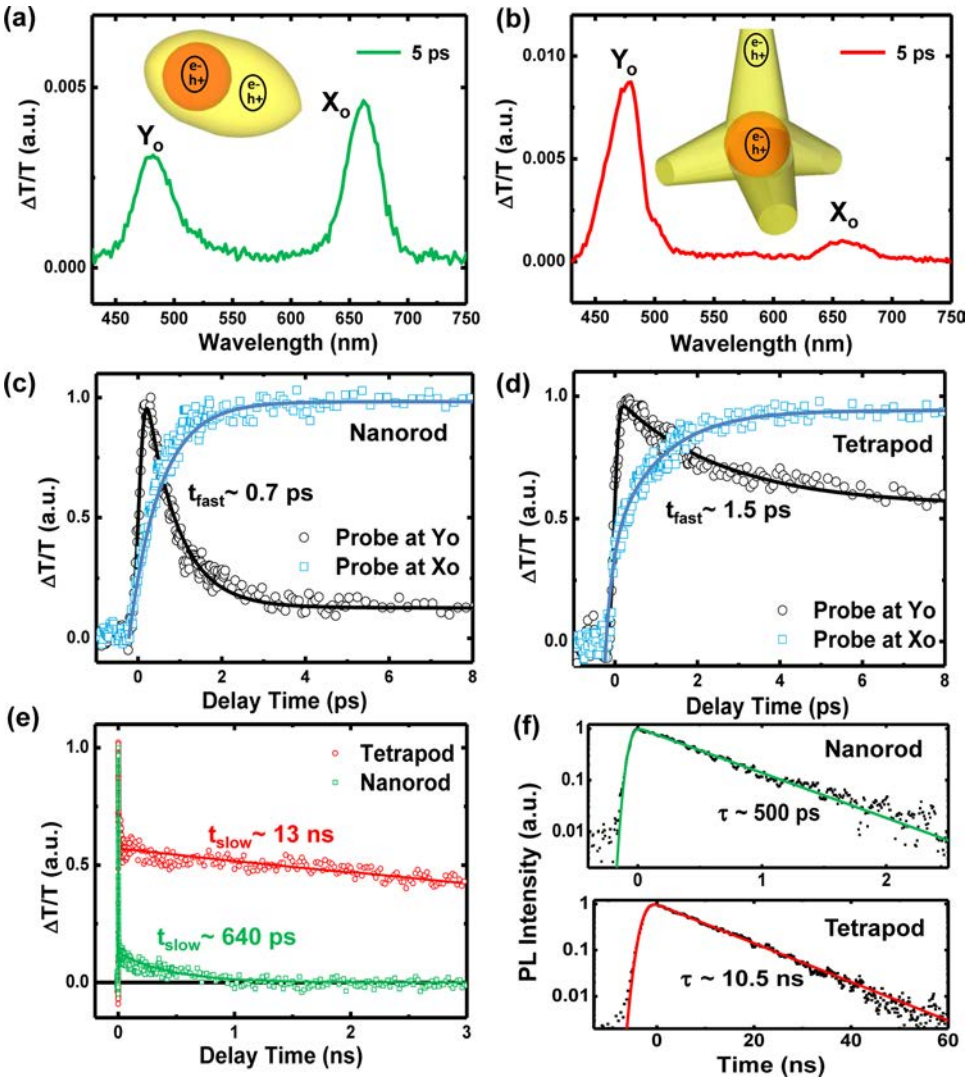

Figure 4. Differential transmission spectra of the CdSe/CdS (a) nanorod and (b) tetrapod samples at a probe delay of 5 ps excited with a 400 nm pulse and pump fluence of 5 μJ/cm^2. Normalized PB transients probed at the peaks of the Y_O and X_O bands for the (c) nanorod and (d) tetrapod samples. (e) Normalized PB transients probed at the peak of Y_O at a longer time scale. (f) Normalized time-resolved PL of CdS emission from nanorods (top panel) and tetrapods (bottom panel) with the pump fluence of 50 μJ/cm^2. Solid lines in (c–f) are fittings with exponential decay functions.

lifetimes of CdS nanocrystals,[31,32] and we may attribute this emission to long-lived excitons localized in CdS *via* surface-trapped carriers. The comparable EL intensity between the CdS and CdSe emission in the tetrapod–LED device may be understood by the creation of more surface trap states during device fabrication.

In contrast, carrier capture from the CdS rod-like shell to the CdSe core in nanorods was much faster at ~0.7 ps (Figure 4c) due to the proximity to the CdSe core and the significantly smaller surface area on a per-particle basis (*i.e.*, smaller surface-to-volume ratio). Indeed, PL emission from CdS in very long CdSe-seeded CdS nanorods was more prominent despite their lower quantum yield with respect to core emission (see Supporting Information). As shown in Figure 4c, the amplitude weightage of the fast decay component of the Y_O bleach is ~90%, which suggests that a larger fraction of the photogenerated charge carriers in the CdS arms is localized to the CdSe core. The remaining carriers give rise to extremely weak CdS emission with subnanosecond lifetime as revealed from the TA and time-resolved PL (TRPL) measurements shown in Figure 4e,f, respectively, which explains why the EL peak at 500 nm in the nanorod–LED device was scarcely detectable (inset, Figure 2a). These results collectively indicate that dual wavelength EL in fluorescent semiconductor nanoheterostructures may be achieved under relatively low electron–hole pair injection rates *via* a judicious combination of nanoparticle structure and surface trap states.

CONCLUSION

In summary, we demonstrated spectrally distinct, dual wavelength EL emission from type I CdSe-seeded CdS tetrapod-based LED devices. Comparable EL intensities were derived from the CdSe core and CdS

arms under relatively low applied bias, which is unexpected since excitons in CdS should rapidly localize to the CdSe core. The origins of the dual wavelength emission were probed by TRPL and TA spectroscopy, which revealed the presence of long-lived excitons in CdS due to surface trap states. On the other hand, CdSe-seeded CdS nanorods with faster and more effective carrier localizations to the core and possibly a lower density of surface trap states did not possess an appreciable fraction of long-lived excitons in the CdS rod-like shell upon photoexcitation and consequently did not exhibit any notable dual wavelength PL as well as EL. These results collectively indicate that dual wavelength EL in fluorescent semiconductor nanoheterostructures may be achieved under relatively low electron–hole pair injection rates *via* a judicious combination of nanoparticle structure and surface trap states.

METHOD

Nanoparticles Synthesis. Briefly, a mixture containing presynthesized CdSe core nanoparticles, elemental sulfur, and trioctylphosphine was swiftly injected at an elevated temperature into a solvent containing cadmium oxide, alkyl phosphonic acids, and/or carboxylic acids which served as surfactants (see Supporting Information for details).

Device Fabrication. In order to fabricate the QD-LED, a prepatterned indium tin oxide (ITO) glass substrate was first etched with HCl (Zn powder as catalyst) and rinsed with deionized (DI) water to form the anode. Upon cleaning with acetone and isopropyl alcohol, the ITO/glass substrate was baked dry and a thin layer of poly(3,4-ethylenedioxythiophene):poly-(styrenesulfonate) (PEDOT:PSS) was spin-coated onto it. The substrate was then annealed at 250 °C for 20 min in a glovebox under 99.9995% argon. Subsequently, CdSe-seeded CdS tetrapods (or nanorods) at a concentration of ~10 mg/mL in toluene were spin-coated onto the substrate (3000 rpm) and dried on a hot plate at ~50 °C. A ~2 nm layer of LiF and ~100 nm of aluminum were consecutively evaporated onto the nanoparticle active layer *via* a shadow mask in order to yield the cathode, and the resulting QD-LED device was packaged in a sealed cover glass before the measurement.

Structural Characterization. A JEOL JEM 1220F (100 kV accelerating voltage) or JEOL JEM 2100 (200 kV accelerating voltage) microscope was used to obtain bright-field TEM images of the nanoparticles. For TEM measurements, a drop of the nanoparticle solution was placed onto a 300 mesh size copper grid covered with a continuous carbon film. Excess solution was removed by an adsorbent paper, and the sample was dried at room temperature.

Optical Characterization. EL measurement was done by applying a constant voltage on the sample from a Keithley 2400 source and measurement unit, and the EL signal was detected by a photomultiplier detector connected to a monochromator and collected *via* an optical fiber. UV–visible absorption spectra were obtained with an Agilent 8453 UV–visible spectrophotometer. Photoluminescence (PL) spectra were collected with a Shimadzu RF-5301PC spectrofluorophotometer. Care was taken to ensure that the concentrations of the core and core-seeded nanostructures were sufficiently diluted to avoid contributions from reabsorption or energy transfer.

For pump-fluence-dependent PL, the laser source was a Coherent Legend regenerative amplifier (150 fs, 1 kHz, 800 nm) that was seeded by a Coherent Vitesse oscillator (100 fs, 80 MHz). The 800 nm wavelength laser pulses were from the regenerative amplifier's output, while the 400 nm wavelength laser pulses were obtained with a BBO doubling crystal. The laser pulses were focused by a lens (f = 25 cm) on the solution sample in a 2 mm thick quartz cell. The emission from the samples was collected at a backscattering angle of 150° by a pair of lenses and into an optical fiber that is coupled to a spectrometer (Acton, Spectra Pro 2500i) to be detected by a charge-coupled device (Princeton Instruments, Pixis 400B). For time-resolved photoluminescence measurement, the temporal evolution of the PL was recorded by an Optronis Optoscope streak camera system which has an ultimate system resolution of 10 ps when operated in the shortest time window of 330 ps.

For the femtosecond transient absorption measurements, the laser source was a Coherent Libra regenerative amplifier (50 fs, 1 kHz, 800 nm) that was seeded by a Coherent Vitesse oscillator (50 fs, 80 MHz). The 400 nm wavelength pump laser pulses were obtained with a BBO doubling crystal. The samples were pumped by 400 nm pump pulse and probed with a white-light continuum generated with a thin sapphire plate (that was focused by a parabolic mirror to a spot of ~20 μm diameter). The linear polarization of the pump pulse was adjusted to be perpendicular to that of the probe pulse with a polarizer and a half-wave plate. The cross-polarization will help eliminate any contribution from coherent artifacts at early times. Pump-induced differential transmission ($\Delta T/T$) of the probe beam was monitored using a monochromator/photomultiplier tube configuration with lock-in detection. The pump beam was chopped at 83 Hz and used as the reference frequency for the lock-in.

Conflict of Interest: The authors declare no competing financial interest.

Acknowledgment. SUTD-MIT IDC research grant is gratefully acknowledged. This work is also supported by the following research grants: NTU start-up grant (M58110068); SPMS collaborative Research Award (M58110090); and the Competitive Research Program (NRF-CRP5-2009-04; NRF-CRP8-2011-07). G.C.X., T.C.S., and Y.C. also acknowledge funding support from the Singapore National Research Foundation (NRF) through the Singapore–Berkeley Research Initiative for Sustainable Energy (SinBeRISE) CREATE Programme.

Supporting Information Available: Detailed synthesis technique and data that are complementary to the paper are given in the Supporting Information. This material is available free of charge *via* the Internet at http://pubs.acs.org.

REFERENCES AND NOTES

1. Green, M. A.; Zhao, J.; Wang, A.; Reece, P. J.; Gal, M. Efficient Silicon Light-Emitting Diodes. *Nature* **2001**, *412*, 805–808.
2. Salter, C. L.; Stevenson, R. M.; Farrer, I.; Nicoll, C. A.; Ritchie, D. A.; Shields, A. J. An Entangled-Light-Emitting Diode. *Nature* **2010**, *465*, 594–597.
3. Kwak, J.; Bae, W. K.; Lee, D.; Park, I.; Lim, J.; Park, M.; Cho, H.; Woo, H.; Yoon, D. Y.; Char, K.; *et al.* Bright and Efficient Full-Color Colloidal Quantum Dot Light-Emitting Diodes Using an Inverted Device Structure. *Nano Lett.* **2012**, *12*, 2362–2366.
4. Pal, B. N.; Ghosh, Y.; Brovelli, S.; Laocharoensuk, R.; Klimov, V. I.; Hollingsworth, J. A.; Htoon, H. 'Giant' CdSe/CdS Core/Shell Nanocrystal Quantum Dots as Efficient Electroluminescent Materials: Strong Influence of Shell Thickness on Light-Emitting Diode Performance. *Nano Lett.* **2012**, *12*, 331–336.
5. Steckel, J. S.; Zimmer, J. P.; Coe-Sullivan, S.; Stott, N. E.; Bulović, V.; Bawendi, M. G. Blue Luminescence from (CdS)ZnS Core–Shell Nanocrystals. *Angew. Chem., Int. Ed.* **2004**, *43*, 2154–2158.
6. Coe-Sullivan, S.; Woo, W.-K.; Steckel, J. S.; Bawendi, M.; Bulović, V. Tuning the Performance of Hybrid

Organic/Inorganic Quantum Dot Light-Emitting Devices. *Org. Electron.* **2003**, *4*, 123–130.
7. Steckel, J. S.; Coe-Sullivan, S.; Bulović, V.; Bawendi, M. G. 1.3 to 1.55 μm Tunable Electroluminescence from PbSe Quantum Dots Embedded within an Organic Device. *Adv. Mater.* **2003**, *15*, 1862–1866.
8. Anikeeva, P. O.; Halpert, J. E.; Bawendi, M. G.; Bulović, V. Quantum Dot Light-Emitting Devices with Electroluminescence Tunable over the Entire Visible Spectrum. *Nano Lett.* **2009**, *9*, 2532–2536.
9. Colvin, V. L.; Schlamp, M. C.; Alivisatos, A. P. Light-Emitting Diodes Made from Cadmium Selenide Nanocrystals and a Semiconducting Polymer. *Nature* **1994**, *370*, 354–357.
10. Dabbousi, B. O.; Bawendi, M. G.; Onitsuka, O.; Rubner, M. F. Electroluminescence from CdSe Quantum-Dot/Polymer Composites. *Appl. Phys. Lett.* **1995**, *66*, 1316–1318.
11. Coe, S.; Woo, W. K.; Bawendi, M.; Bulovic, V. Electroluminescence from Single Monolayers of Nanocrystals in Molecular Organic Devices. *Nature* **2002**, *420*, 800–803.
12. Anikeeva, P. O.; Madigan, C. F.; Halpert, J. E.; Bawendi, M. G.; Bulović, V. Electronic and Excitonic Processes in Light-Emitting Devices Based on Organic Materials and Colloidal Quantum Dots. *Phys. Rev. B* **2008**, *78*, 085434.
13. Anikeeva, P. O.; Madigan, C. F.; Coe-Sullivan, S. A.; Steckel, J. S.; Bawendi, M. G.; Bulović, V. Photoluminescence of CdSe/ZnS Core/Shell Quantum Dots Enhanced by Energy Transfer from a Phosphorescent Donor. *Chem. Phys. Lett.* **2006**, *424*, 120–125.
14. Clapp, A. R.; Medintz, I. L.; Mauro, J. M.; Fisher, B. R.; Bawendi, M. G.; Mattoussi, H. Fluorescence Resonance Energy Transfer between Quantum Dot Donors and Dye-Labeled Protein Acceptors. *J. Am. Chem. Soc.* **2003**, *126*, 301–310.
15. Shirasaki, Y.; Supran, G. J.; Tisdale, W. A.; Bulović, V. Origin of Efficiency Roll-Off in Colloidal Quantum-Dot Light-Emitting Diodes. *Phys. Rev. Lett.* **2013**, *110*, 217403.
16. Wang, T.; Zhuang, J.; Lynch, J.; Chen, O.; Wang, Z.; Wang, X.; LaMontagne, D.; Wu, H.; Wang, Z.; Cao, Y. C. Self-Assembled Colloidal Superparticles from Nanorods. *Science* **2012**, *338*, 358–363.
17. Rizzo, A.; Nobile, C.; Mazzeo, M.; Giorgi, M. D.; Fiore, A.; Carbone, L.; Cingolani, R.; Manna, L.; Gigli, G. Polarized Light Emitting Diode by Long-Range Nanorod Self-Assembling on a Water Surface. *ACS Nano* **2009**, *3*, 1506–1512.
18. Lutich, A. A.; Mauser, C.; Da Como, E.; Huang, J.; Vaneski, A.; Talapin, D. V.; Rogach, A. L.; Feldmann, J. Multiexcitonic Dual Emission in CdSe/CdS Tetrapods and Nanorods. *Nano Lett.* **2010**, *10*, 4646–4650.
19. Xu, Y.; Lian, J.; Mishra, N.; Chan, Y. Multifunctional Semiconductor Nanoheterostructures *via* Site-Selective Silica Encapsulation. *Small* **2013**, *9*, 1908–1915.
20. Fiore, A.; Mastria, R.; Lupo, M. G.; Lanzani, G.; Giannini, C.; Carlino, E.; Morello, G.; De Giorgi, M.; Li, Y.; Cingolani, R.; *et al.* Tetrapod-Shaped Colloidal Nanocrystals of II–VI Semiconductors Prepared by Seeded Growth. *J. Am. Chem. Soc.* **2009**, *131*, 2274–2282.
21. Talapin, D. V.; Nelson, J. H.; Shevchenko, E. V.; Aloni, S.; Sadtler, B.; Alivisatos, A. P. Seeded Growth of Highly Luminescent CdSe/CdS Nanoheterostructures with Rod and Tetrapod Morphologies. *Nano Lett.* **2007**, *7*, 2951–2959.
22. Mauser, C.; Limmer, T.; Da Como, E.; Becker, K.; Rogach, A. L.; Feldmann, J.; Talapin, D. V. Anisotropic Optical Emission of Single CdSe/CdS Tetrapod Heterostructures: Evidence for a Wavefunction Symmetry Breaking. *Phys. Rev. B* **2008**, *77*, 153303.
23. Xing, G.; Liao, Y.; Wu, X.; Chakrabortty, S.; Liu, X.; Yeow, E. K. L.; Chan, Y.; Sum, T. C. Ultralow-Threshold Two-Photon Pumped Amplified Spontaneous Emission and Lasing from Seeded CdSe/CdS Nanorod Heterostructures. *ACS Nano* **2012**, *6*, 10835–10844.
24. Carbone, L.; Nobile, C.; De Giorgi, M.; Sala, F. D.; Morello, G.; Pompa, P.; Hytch, M.; Snoeck, E.; Fiore, A.; Franchini, I. R.; *et al.* Synthesis and Micrometer-Scale Assembly of Colloidal CdSe/CdS Nanorods Prepared by a Seeded Growth Approach. *Nano Lett.* **2007**, *7*, 2942–2950.
25. Mishra, N.; Lian, J.; Chakrabortty, S.; Lin, M.; Chan, Y. Unusual Selectivity of Metal Deposition on Tapered Semiconductor Nanostructures. *Chem. Mater.* **2012**, *24*, 2040–2046.
26. Zhang, X.; Chen, Y. L.; Liu, R.-S.; Tsai, D. P. Plasmonic Photocatalysis. *Rep. Prog. Phys.* **2013**, *76*, 046401.
27. Empedocles, S. A.; Bawendi, M. G. Quantum-Confined Stark Effect in Single CdSe Nanocrystallite Quantum Dots. *Science* **1997**, *278*, 2114–2117.
28. Sitt, A.; Della Sala, F.; Menagen, G.; Banin, U. Multiexciton Engineering in Seeded Core/Shell Nanorods: Transfer from Type-I to Quasi-type-II Regimes. *Nano Lett.* **2009**, *9*, 3470–3476.
29. Wu, K. F.; Rodriguez-Cordoba, W. E.; Liu, Z.; Zhu, H. M.; Lian, T. Q. Beyond Band Alignment: Hole Localization Driven Formation of Three Spatially Separated Long-Lived Exciton States in CdSe/CdS Nanorods. *ACS Nano* **2013**, *7*, 7173–7185.
30. Mauser, C.; Da Como, E.; Baldauf, J.; Rogach, A. L.; Huang, J.; Talapin, D. V.; Feldmann, J. Spatio-temporal Dynamics of Coupled Electrons and Holes in Nanosize CdSe–CdS Semiconductor Tetrapods. *Phys. Rev. B* **2010**, *82*, 081306.
31. Lakowicz, J. R.; Gryczynski, I.; Gryczynski, Z.; Murphy, C. J. Luminescence Spectral Properties of CdS Nanoparticles. *J. Phys. Chem. B* **1999**, *103*, 7613–7620.
32. Zhao, H.; Chaker, M.; Wu, N.; Ma, D. Towards Controlled Synthesis and Better Understanding of Highly Luminescent PbS/CdS Core/Shell Quantum Dots. *J. Mater. Chem.* **2011**, *21*, 8898–8904.

Supporting Information for

Dual Wavelength Electroluminescence from CdSe/CdS Tetrapods

Jen It Wong[†,§], Nimai Mishra[‡,§], Guichuan Xing[ǁ#], Mingjie Li[‡], Sabyasachi Chakrabortty[‡], Tze Chien Sum[ǁ#], Yumeng Shi[†], Yinthai Chan[*,‡,⊥] and Hui Ying Yang[*,†]

[†]*Pillar of Engineering Product Development, Singapore University of Technology and Design, 20 Dover Drive, Singapore 138682.*
[‡]*Department of Chemistry, National University of Singapore, 3 Science Drive 3, Singapore 117543*
[ǁ]*School of Physical & Mathematical Sciences, Nanyang Technological University, 21 Nanyang Link, Singapore 637371*
 # Singapore-Berkeley Research Initiative for Sustainable Energy, 1 Create Way, 138602, Singapore
[⊥]*Institute for Materials Research & Engineering, A*STAR, 3 Research Link, Singapore 117602*

Chemicals for nanoparticles synthesis:

Cadmium acetylacetonate (Cd(acac)2, 99.9%), cadmium oxide (CdO, 99.5%), dodecylamine (DDA, 98%), 1,2-hexadecanediol (HDDO, 90%), 1-hexadecylamine (HDA, 90%), 1-octadecene (ODE, 90%), sulfur (S, reagent grade), selenium (Se, 99.99%), oleic acid (OA, 90%), myristic acid (MA, 99%), trioctylphosphine oxide (TOPO, 90%), and oleylamine (technical grade, 70%) were purchased from Sigma Aldrich. Trioctylphosphine (TOP, 97%) was purchased from Alfa Aesar.. n-octadecylphosphonic acid (ODPA, 97%), n-hexylphosphonic acid (HPA, 97%) and trioctylphosphine oxide (TOPO, 99%) were purchased from Strem. All the chemicals were used as received without further purification. Unless stated otherwise, all the reactions were conducted in oven-dried glassware under nitrogen atmosphere using standard Schlenk techniques.

Materials for device fabrication:

Indium tin oxide(ITO) glass, Hydrochloric acid (HCl), Zinc (powder, 99.995%), Lithium fluoride (LiF) , Aluminium (Al), poly(3,4-ethylenedioxythiophene):poly(styrenesulfonate)

(PEDOT:PSS)

Synthesis of Spherical Wurtzite CdSe Seeds:

Synthesis of monodispersed w-CdSe NCs proceeded *via* a previously reported procedure with slight modifications.[1] A bath of 6 g of TOPO (90%), 3g of TOPO (99%) and 6 g of HAD was degassed at 100 °C for 1.5 h. A precursor solution comprising 317 mg of $Cd(acac)_2$ and 567 mg of HDDO in 6 mL of ODE was degassed at 120 °C for 1.5 h, followed by addition of 2 mL of 1.5 M trioctylphosphine selenide at room temperature. This precursor solution was then rapidly injected into the bath at 360 °C and allowed to cool to 80 °C. The resulting CdSe NCs were subsequently processed by 3 cycles of precipitation in a butanol/methanol mixture and redispersed in toluene for further use.

Synthesis of Spherical Zinc Blende CdSe Seeds:

Nearly monodispersed zb-CdSe nanocrystals (NCs) were synthesized *via* a previously reported method.[2] In a 50 mL three-neck round-bottom flask, 0.3 mmol CdO, 0.6 mmol myristic acid and 5 mL of 1-ODE were degassed at 90 °C for about 1 h. The solution was then heated to 250 °C for ∼10−15 min to yield a clear solution, followed by the addition of 7 mL of ODE before cooling to 90 °C to degas for another 1 h. Upon cooling to room temperature, 0.012 g (0.15 mmol) of 100 mesh Se powder (99.999%) was added to the reaction mixture and degassed at 50°C for ∼20 min. Upon heating to 240 °C under N_2, a color change from colorless to yellow at ∼150°C and then to orange-red color upon reaching 240°C were observed, signifying the formation of zb-CdSe nuclei. A degassed mixture of 0.05 mL of oleic acid and 0.5 mL of oleylamine in 2 mL of 1-ODE was subsequently added dropwise to the reaction mixture. From our observation we found that the growth time for a ∼5-6 nm diameter NC was approximately 2 h. As-synthesized zb-CdSe NCs were precipitated out from the growth solution by adding

acetone, and were subsequently allowed to undergo two more cycles of redispersion and precipitation in toluene and methanol respectively.

Preparation of Stock Solution of CdSe Seeds:

Processed CdSe NCs (zb/w) were dispersed in a minimum amount of toluene and their concentration was determined by measuring their absorbance at 350 nm, whose molar absorptivity is known.[3] The toluene was then removed under vacuum and TOP was added to make up a NC concentration of 100 μM. This mixture will subsequently be referred to as the zb- or w-CdSe stock solution.

Synthesis of CdSe-Seeded CdS nanorod and tetrapods:

For the synthesis of nanorods, wurtzite- CdSe (W-CdSe) nanoparticle seeds were first injected into a mixture of surfactant, surface ligand and Cd-precursor at 360^{o} C and allowed to grow for few minutes. The W-CdSe core was synthesized by previously reported method.[1] The low resolution Transmission Electron Microscope (TEM) images show the W-CdSe of highly mono-disperse in size with average diameter ~5.5 nm. (Fig. S1a) The CdSe seeded CdS nanorods used in this study were synthesized using the seeded growth approach of Manna *et al.* with slight modifications.[4] The length of the nanorods can be tuned by changing either the core concentration or precursor concentration while keeping other parameters the same. Relatively monodisperse nanorods of two different lengths were produced, the shorter nanorods possessed an average length and diameter of ~39 nm and ~18 nm respectively with a size distribution of less than 3% while the longer nanorods were found to have an average length and diameter of ~157 nm and ~6 nm with less than 5% size distribution. The yield of nanorods was very high at ~ 90%, with negligible numbers of branched structures as side products, thus obviating the need for post-synthetic processing. From the UV-vis and emission spectra of our sample (Fig. S1b)

starting from the core to short and long nanorods in the toluene solvent, the absorbance features in W-CdSe sample also conclude the very good size distribution of the sample. Upon growth of CdS on the W-CdSe seeds the main absorbance contribution comes from the CdS arm, it can be understood by the fact that volume fraction of the CdS arm is very high comparable to the core. The red shift in the emission spectra observed because of delocalization of the electronic wave function to the shell. The CdS optical features in the case of long rod can be understood by strong quantum confinement in the diameter.

On the other hand, the Zb CdSe seeded CdS tetrapods were synthesized from previously reported methods[5], in brief Zb CdSe was injected with the TOPS in a mixture of oleic acid (OA) and octadecylphosphonic acid (ODPA) was used as surfactants instead of octadecylphosphonic acid (ODPA) and HPA (for details see table below). While Zb CdSe core synthesized from the reported methods by Cao *et al.* [2] It can clearly be seen from Fig. S2a that the highly mono-disperse Zb CdSe of ~ 5.4 nm diameter in size. This allowed for mono-disperse tetrapods of various arm dimensions with yields as high as 95% (with respect to nanorods, bipod and tripod by-products) to be obtained, which may be attributed to the stabilization of the zinc blende phase of CdSe by OA.[6] The average arm length of the tetrapods were found to be ~27 nm . The absorbance and emission spectra of the as synthesized sample from tetrapods in toluene were shown in Fig. S2b.

In short, rodlike and tetrapod-like CdSe-seeded CdS heterostructures were synthesized *via* the seeded growth approach.[5, 7] Briefly, 3 g of TOPO (99%) for nanorod (2.65 g of TOPO (99%) for tetrapods), desired amount of CdO, and a mixture of ligands were degassed at 150 °C for about 1.5 h in a 50 mL three-neck round bottom flask. The reaction mixture was then heated to 350 °C under N_2, whereupon the solution turned from reddish brown to colorless. Separately,

a mixture of S, TOP, and CdSe seeds was derived by first dissolving a predetermined amount of S in TOP at 50 °C before adding 25 μL of the appropriate CdSe stock solution. Upon reaching the desired injection temperature (which is 350 °C for both case), an additional amount of TOP was added (1.8 and 0.9 mL in the case of nanorods and tetrapods respectively), and the temperature was allowed to recover to 350 °C before the mixture of S, TOP, and CdSe was swiftly injected. The temperature was again allowed to recover to 350 °C and the anisotropic CdS shell (or arms in the case of tetrapods) was grown at this temperature for "t" minutes. The heating mantle was then removed and the solution was allowed to cool to 80 °C. As-synthesized CdSe seeded CdS nanorods/tetrapods were then processed by repeated cycles of precipitation in methanol and redispersion in toluene. A summary of the reaction conditions used for synthesis different kind of nanorod and tetrapods used in this work is given in Table below.

Table S1 Detailed Synthesis of CdSe seeded CdS nanoheterostructures:

CdSe seeded CdS rods/tetrpods	Amount of CdSe core added	Amounts of ligand added	Amounts of CdO added	Amount of sulfur in TOP	Growth time, *t* (min)
Nanorods	16×10^{-9} mol (w-CdSe)	ODPA (30 mg) HPA (70 mg)	0.05 g	TOP (1.8 mL), S (70 mg)	6
Tetrapods	2.5×10^{-9} mol (zb-CdSe)	ODPA (140mg), OA (0.5 mL)	0.052 g	TOP (0.6 mL), S (7 mg)	10
Long Nanorods	10×10^{-9} mol (w-CdSe)	HPA (80 mg) ODPA (290 mg)	0.09 g	TOP (1.8 mL), S (120 mg)	8

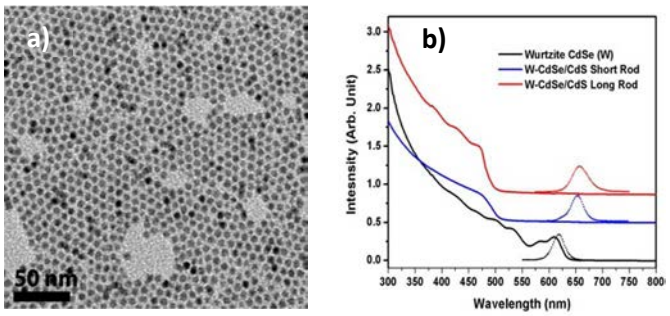

Figure S1 (a) TEM image of as synthesized W-CdSe core. (b) Optical spectra of short and long CdSe seeded CdS nanorod from the same core.

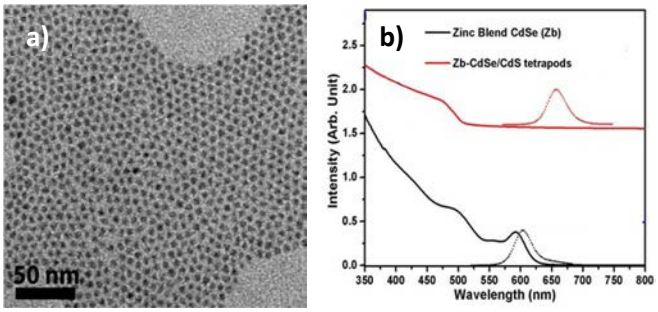

Figure S2 (a) TEM image of as synthesized zb-CdSe core. (b) Optical spectra of CdSe seeded CdS tetrapods from the same core.

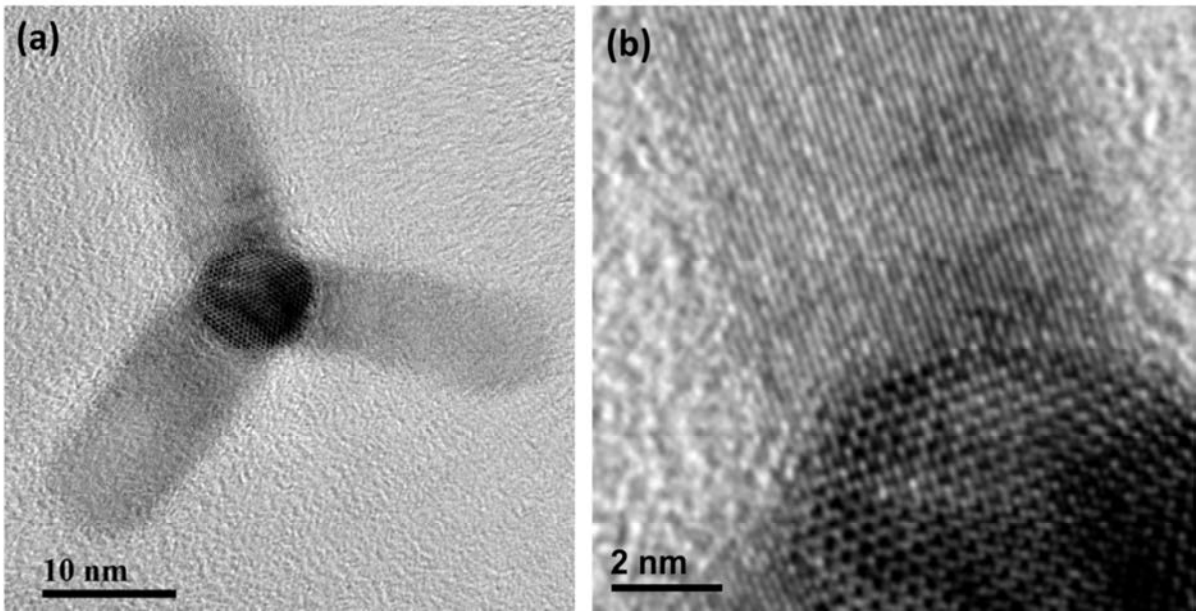

Figure S3 (a) TEM image of a typical CdSe/CdS tetrapod. (b) HRTEM images of the interface between CdSe and CdS where the lattice fringes of the fourth arm perpendicular to the substrate can be seen.

Figure S3 above are HRTEM images of typical CdSe/CdS tetrapods, where the lattice fringes of the fourth arm perpendicular to the substrate can be seen. Due to the geometry of the structure, direct imaging of the CdSe core is not possible as it is always obstructed by the CdS arm that points in the same direction as the electron beam. Intimate contact between CdSe and CdS is generally inferred from the stead state absorption/emission spectra which shows a significant redshift of the CdSe core absorption/emission upon coating with CdS. In order to avoid any unambiguity, we have included the absorption/emission spectrum of the CdSe core (before CdS arm growth) in the Supporting Information as well.

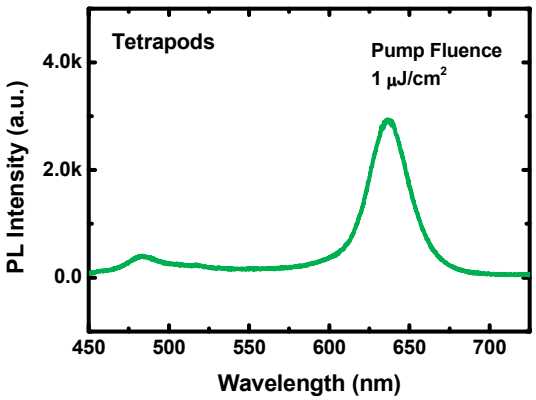

Figure S4 A relatively weak CdS PL was observed in the case of CdSe seeded CdS tetrapods under the relatively low optical pump intensities akin to the typical rates of electron/hole injection in an LED device.

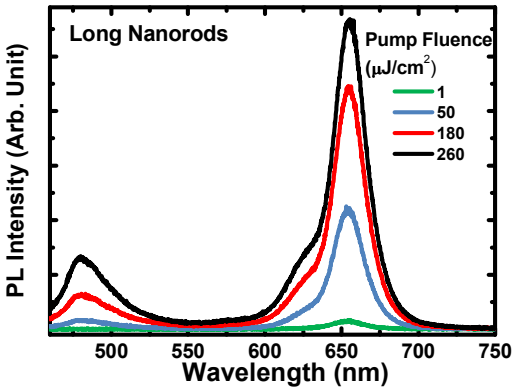

Figure S5 Photoluminescence(PL) spectra from long nanorods. The PL from CdS in very long CdSe seeded CdS nanorods was more prominent compared to short nanorods.

References:

1. Snee, P. T.; Chan, Y.; Nocera, D. G.; Bawendi, M. G. Whispering-Gallery-Mode Lasing from a Semiconductor Nanocrystal/Microsphere Resonator Composite. *Adv. Mater.* **2005**, 17, 1131-1136.
2. Yang, Y. A.; Wu, H.; Williams, K. R.; Cao, Y. C. Synthesis of CdSe and CdTe Nanocrystals without Precursor Injection. *Angew. Chem. Int. Ed.* **2005**, 44, 6712-6715.
3. Leatherdale, C. A.; Woo, W. K.; Mikulec, F. V.; Bawendi, M. G. On the Absorption Cross Section of CdSe Nanocrystal Quantum Dots. *J. Phys. Chem. B* **2002**, 106, 7619-7622.
4. Carbone, L.; Nobile, C.; De Giorgi, M.; Sala, F. D.; Morello, G.; Pompa, P.; Hytch, M.; Snoeck, E.; Fiore, A.; Franchini, I. R.*; et al.* Synthesis and Micrometer-Scale Assembly of Colloidal CdSe/CdS Nanorods Prepared by a Seeded Growth Approach. *Nano Lett.* **2007**, 7, 2942-2950.
5. Mishra, N.; Lian, J.; Chakrabortty, S.; Lin, M.; Chan, Y. Unusual Selectivity of Metal Deposition on Tapered Semiconductor Nanostructures. *Chem. Mater.* **2012**, 24, 2040-2046.
6. Mahler, B.; Lequeux, N.; Dubertret, B. Ligand-Controlled Polytypism of Thick-Shell CdSe/CdS Nanocrystals. *J. Am. Chem. Soc.* **2009**, 132, 953-959.
7. Talapin, D. V.; Nelson, J. H.; Shevchenko, E. V.; Aloni, S.; Sadtler, B.; Alivisatos, A. P. Seeded Growth of Highly Luminescent CdSe/CdS Nanoheterostructures with Rod and Tetrapod Morphologies. *Nano Lett.* **2007**, 7, 2951-2959.